SUPPORTING INFORMATION

Ligand effects on the $[Cu(PhO)(PhOH)]^+$ redox active complex

Elixabete Rezabal,[1] Lucie Ducháčková,[2] Petr Milko,[3] Max C. Holthausen,[*1] and Jana Roithová[*2]

[1]*Institut für Anorganische und Analytische Chemie, Johann Wolfgang Goethe-Universität Frankfurt, Max-von-Laue-Straße 7, 60438 Frankfurt am Main, Germany,* [2]*Charles University in Prague, Faculty of Science, Department of Organic and Nuclear Chemistry Hlavova 8, 12840 Praha 2, Czech Republic, and* [3]*Institute of Organic Chemistry and Biochemistry, Flemingovo nám. 2, 16610 Prague 6, Czech Republic*

E-mails: roithova@natur.cuni.cz, max.holthausen@chemie.uni-frankfurt.de

Experimental Details

Table S1. Experimental binding energies of the phenoxy radical and ligands L in $[Cu(PhO)(L)]^+$ in eV.[a]

L	Collision gas	MWHM[b]	N_{vib}[c]	N_{rot}[d]	AE_{exp} (-PhO)[e]	AE_{exp} (-L)[e]
H_2O	Ar	2	42	3	2.4 ± 0.2	1.6 ± 0.1
	Xe	1.2			2.6 ± 0.1	1.3 ± 0.1
					2.5 ± 0.3	**1.5 ± 0.3**
CH_3OH	Ar	2	51	4	2.2 ± 0.3	1.4 ± 0.1
	Xe	1.2			2.3 ± 0.1	1.5 ± 0.1
					2.2 ± 0.3	**1.4 ± 0.2**
THF	Xe	1.2	72	3	**2.1 ± 0.2**	**1.9 ± 0.2**
Thiophene	Xe	1.2	60	3	**2.0 ± 0.2**	**1.7 ± 0.2**
dme	Ar	2	81	4	1.7 ± 0.1	1.9 ± 0.1
	Xe	1.2			1.7 ± 0.1	2.1 ± 0.1
					1.7 ± 0.1	**2.0 ± 0.2**
NH_3	Ar	2	45	3	1.8 ± 0.1	1.8 ± 0.1
	Xe	1.2			2.1 ± 0.1	2.0 ± 0.1
					1.9 ± 0.2	**1.9 ± 0.2**
Pyrrole	Xe	1.2	63	3	**1.9 ± 0.2**	**2.1 ± 0.2**
pyridine	Ar	2	66	3	1.9 ± 0.1	2.0 ± 0.1
	Xe	1.2			2.1 ± 0.1	2.3 ± 0.1
					2.0 ± 0.2	**2.1 ± 0.2**
imidazole	Ar	2	60	3	1.9 ± 0.1	2.4 ± 0.1
	Xe	1.2			2.1 ± 0.1	2.5 ± 0.1
					2.0 ± 0.2	**2.4 ± 0.2**
TMEDA	Ar	2	105	6	1.7 ± 0.1	(2.1 ± 0.1)[f]
	Xe	1.2			1.8 ± 0.1	(2.6 ± 0.1)[f]
					1.7 ± 0.2	(**2.3 ± 0.3**)[f]

[a] Temperature used in by the L-CID program is set to 473.15 K and the number of collisions used is 25 000. [b] FWHM stands for the full width at half of the maximum of the kinetic energy resolution determined from the retarding-potential analysis of a parent-ion intensity. [c] Number of degrees of freedom. [d] Number of free rotations. [e] Binding energies determined by the L-CID program. [f] Number is related to the energy necessary for the formation of iminium ion from the TMEDA ligand.

General procedure for determination of the binding energies.

1. The collision-energy dependent relative cross sections were measured at least three times for each channel and average is used for further evaluation (open symbols in Figures below).

2. Each curve representing a relative fragmentation cross section determined in CID with argon has been first modeled by double Boltzmann sigmoid curve in order to suppress the experimental noise of the curves used for the L-CID fitting (red lines in Figures S1 – S7 below). The raw data were taken for the L-CID fitting determined in the CID experiment with xenon.

3. The smoothed curves were submitted for the L-CID fitting. Losses of both ligands were fitted at once as well as each separately (blue and green lines in Figures S1 – S7 below). In the case of the CID experiment with xenon, individual channels were fitted separately.

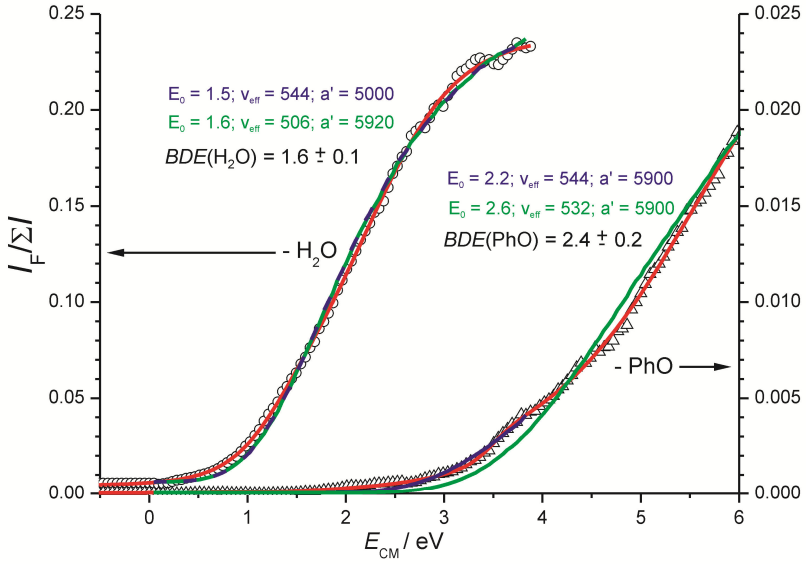

Figure S1. Relative cross sections for the H_2O and PhO losses from the $[Cu(PhO)(H_2O)]^+$ complex upon collision with argon. The open symbols show averages of three measurements. The red lines show curves, which were submitted for the L-CID fitting. The blue curves show the result of parallel fitting of both fragmentation channels. The green lines show separate fittings of the fragmentation channels. The results of the fittings are written in the respective colors.

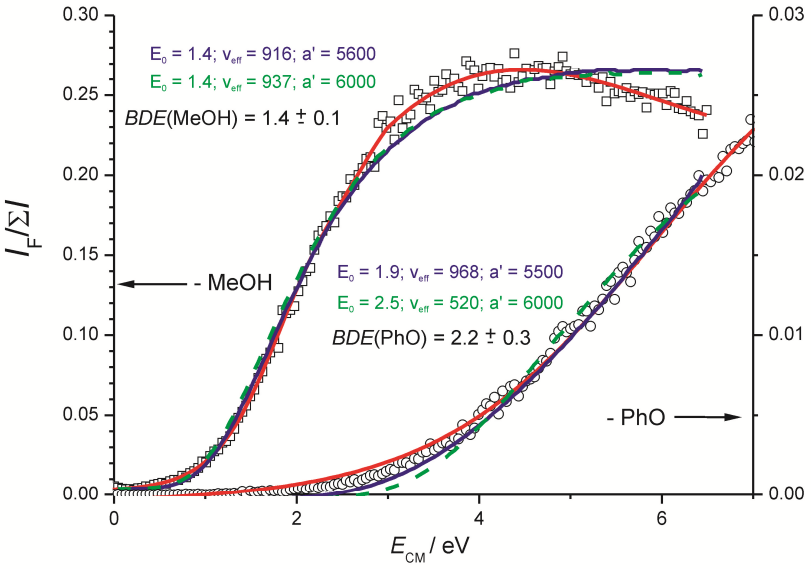

Figure S2. Relative cross sections for the CH_3OH and PhO losses from the $[Cu(PhO)(CH_3OH)]^+$ complex upon collision with argon. The open symbols show averages of two measurements for the loss of methanol and four measurements for the loss of the phenoxy ligand. The red lines show curves, which were submitted for the L-CID fitting. The blue curves show the result of a parallel fitting of both fragmentation channels. The green dashed lines show separate fittings of the fragmentation channels. The results of the fittings are written in the respective colors.

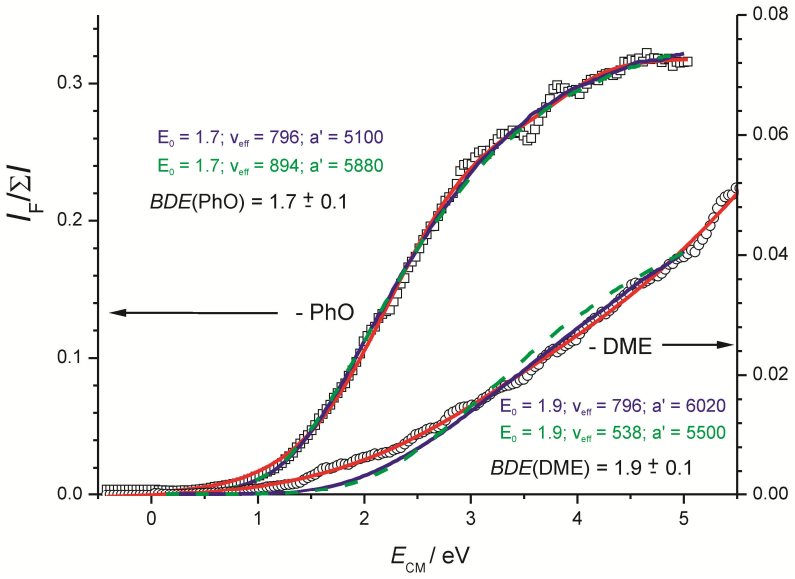

Figure S3. Relative cross sections for the DME and PhO losses from the $[Cu(PhO)(DME)]^+$ complex upon collision with argon. The open symbols show averages of two measurements for the loss of PhO and three measurements for the loss of DME. The red lines show curves, which were submitted for the L-CID fitting. The blue curves show the result of a parallel fitting of both fragmentation channels. The green dashed lines show separate fittings of the fragmentation channels. The results of the fittings are written in the respective colors.

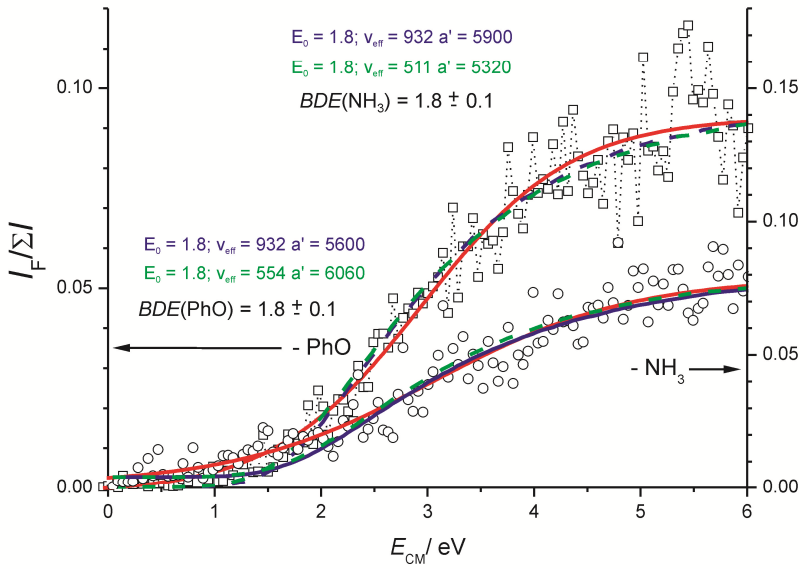

Figure S4. Relative cross sections for the NH_3 and PhO losses from the $[Cu(PhO)(NH_3)]^+$ complex upon collision with argon. The open symbols show averages of three measurements. The red lines show curves, which were submitted for the L-CID fitting. The blue curves show the result of a parallel fitting of both fragmentation channels. The green lines show separate fittings of the fragmentation channels. The results of the fittings are written in the respective colors.

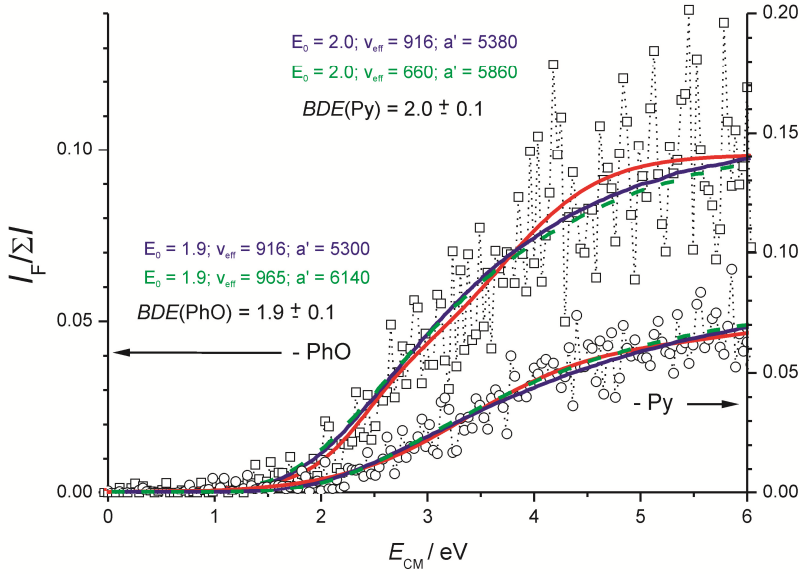

Figure S5. Relative cross sections for the pyridine and PhO losses from the $[Cu(PhO)(Py)]^+$ complex upon collision with argon. The open symbols and black dotted lines show averages of four measurements. The red dotted lines show curves, which were submitted for the L-CID fitting. The blue curves show the result of parallel fitting of both fragmentation channels. The green lines show separate fittings of the fragmentation channel. The results of the fittings are written in the respective colors.

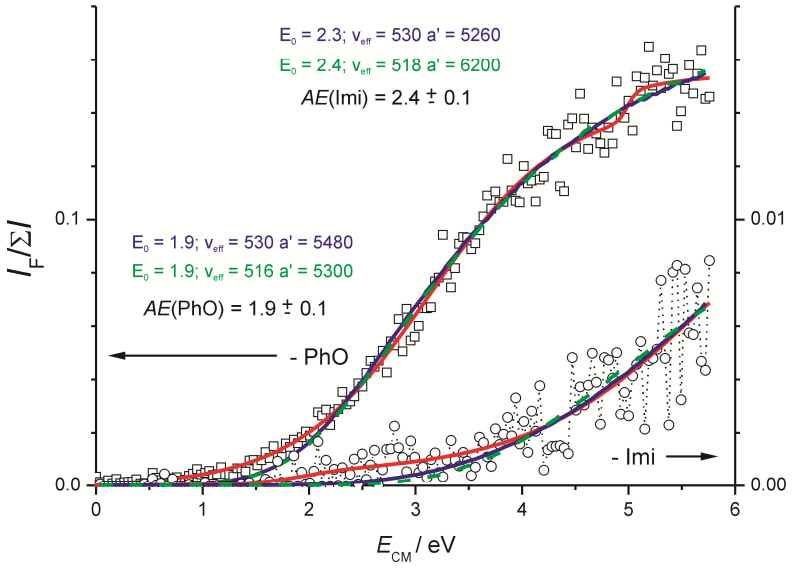

Figure S6. Relative cross sections for the imidazole and PhO losses from the $[Cu(PhO)(Imi)]^+$ complex upon collision with argon. The open symbols show averages of three measurements. The red lines show curves, which were submitted for the L-CID fitting. The blue curves show the result of parallel fitting of both fragmentation channels. The green lines show separate fittings of the fragmentation channels. The results of the fittings are written in the respective colors.

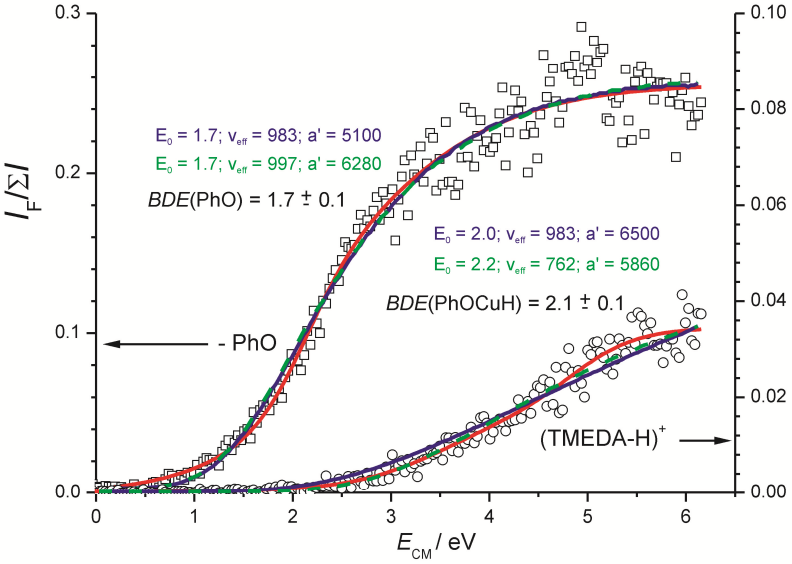

Figure S7. Relative cross sections for the (PhO)CuH and PhO losses from the $[Cu(PhO)(TMEDA)]^+$ complex upon collision with argon. The open symbols show an average of three measurements for the loss of (PhO)CuH and a measurement for the loss of PhO. The red lines show curves, which were submitted for the L-CID fitting. The blue curves show the result of parallel fitting of both fragmentation channels. The green lines show separate fittings of the fragmentation channels. The results of the fittings are written in the respective colors.

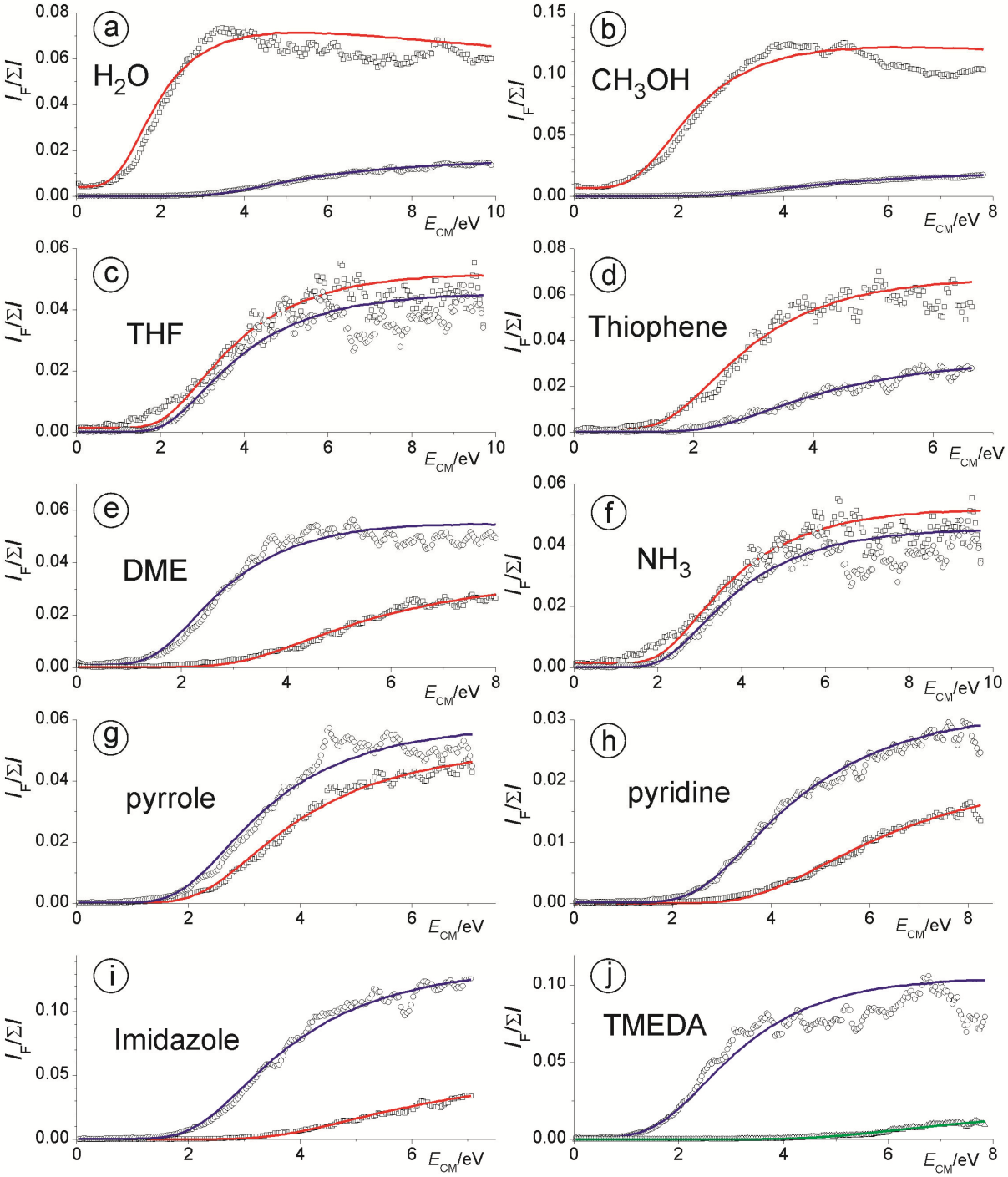

Figure S8. Relative cross sections for the PhO (circle symbols) and L (rectangular symbols) losses from the $[Cu(PhO)(L)]^+$ complex upon collision with xenon; L = H_2O (a), CH_3OH (b), THF (c), thiophene (d), DME (e), NH_3 (f), pyrrole (g), pyridine (h), imidazole (i), and TMEDA (j). The blue lines show the result of the L-CID fitting of the phenoxy-loss channel and the red lines are fits of the L-loss channel. Note that in the case of $[Cu(PhO)(TMEDA)]^+$, the [Cu(PhO)(H)] is lost rather than TMEDA (in green color).

Table S2. Results of the L-CID fitting of the relative fragmentation cross sections of $[Cu(PhO)(L)]^+$ (L = H_2O, CH_3OH, THF, thiophene, DME, NH_3, pyrrole, pyridine, imidazole, and TMEDA) upon CID with xenon. The kinetic energy distribution of the parent ions was 1.2 eV (FWHM)[a] and temperature was set to 473.15 K,

	BDE(PhO)	*BDE*(L)	n_{eff}(PhO)	a'(PhO)	n_{eff} (L)	a' (L)	N_{vib}	N_{rot}
H_2O	2.6	1.3	647	6100	823	5740	42	3
CH_3OH	2.3	1.5	548	6060	771	5740	51	4
THF	2.1	1.9	550	5860	926	5660	72	3
Thiophene	2.0	1.7	547	5380	873	5840	60	3
DME	1.7	2.1	974	5740	514	5300	81	4
NH_3	2.0	2.0	899	5780	751	5660	45	3
Pyrrole	1.9	2.1	928	5600	978	5980	63	3
Pyridine	2.1	2.3	578	6280	544	5480	66	3
Imidazole	2.1	2.5	744	6500	555	6380	60	3
TMEDA	1.8	2.6	562	5920	766	6260	105	6

[a] We have used the energy distribution of 1.2 eV as it is found in the experiment and did not enlarge it to 2 eV as for the fitting of experimental data from the experiment with argon. The effect is negligible.

Results of the DFT Calculations

Figure S9. Isomers of $[Cu(PhO)(L)]^+$ complexes for L = imidazole, pyridine, pyrrole, and thiophene (ZPVE corrected relative energies in eV).

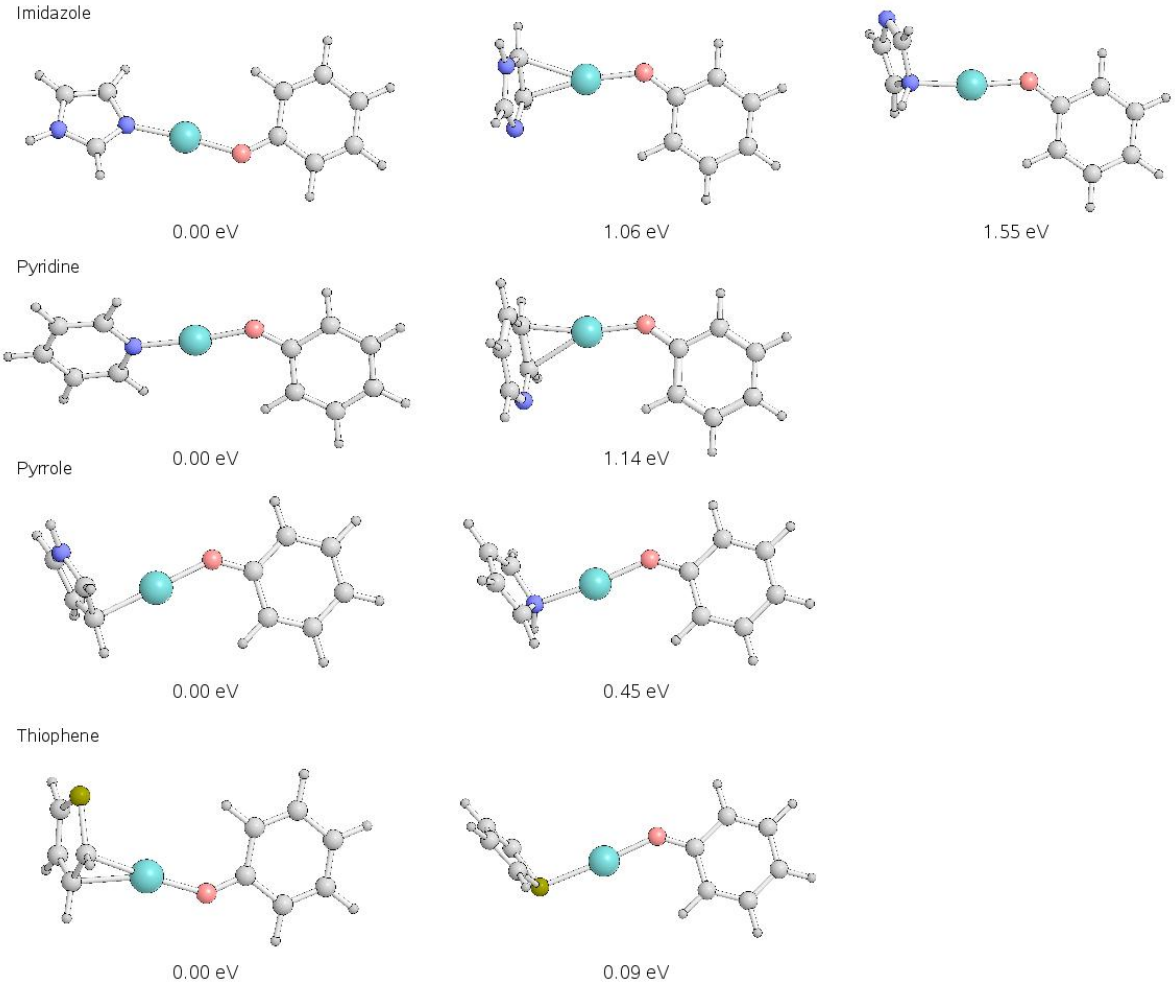

Figure S10. Selected molecular orbitals of complexes $[(L)Cu(PhO)]^+$ for L = NH_3(left) and imidazole (right).

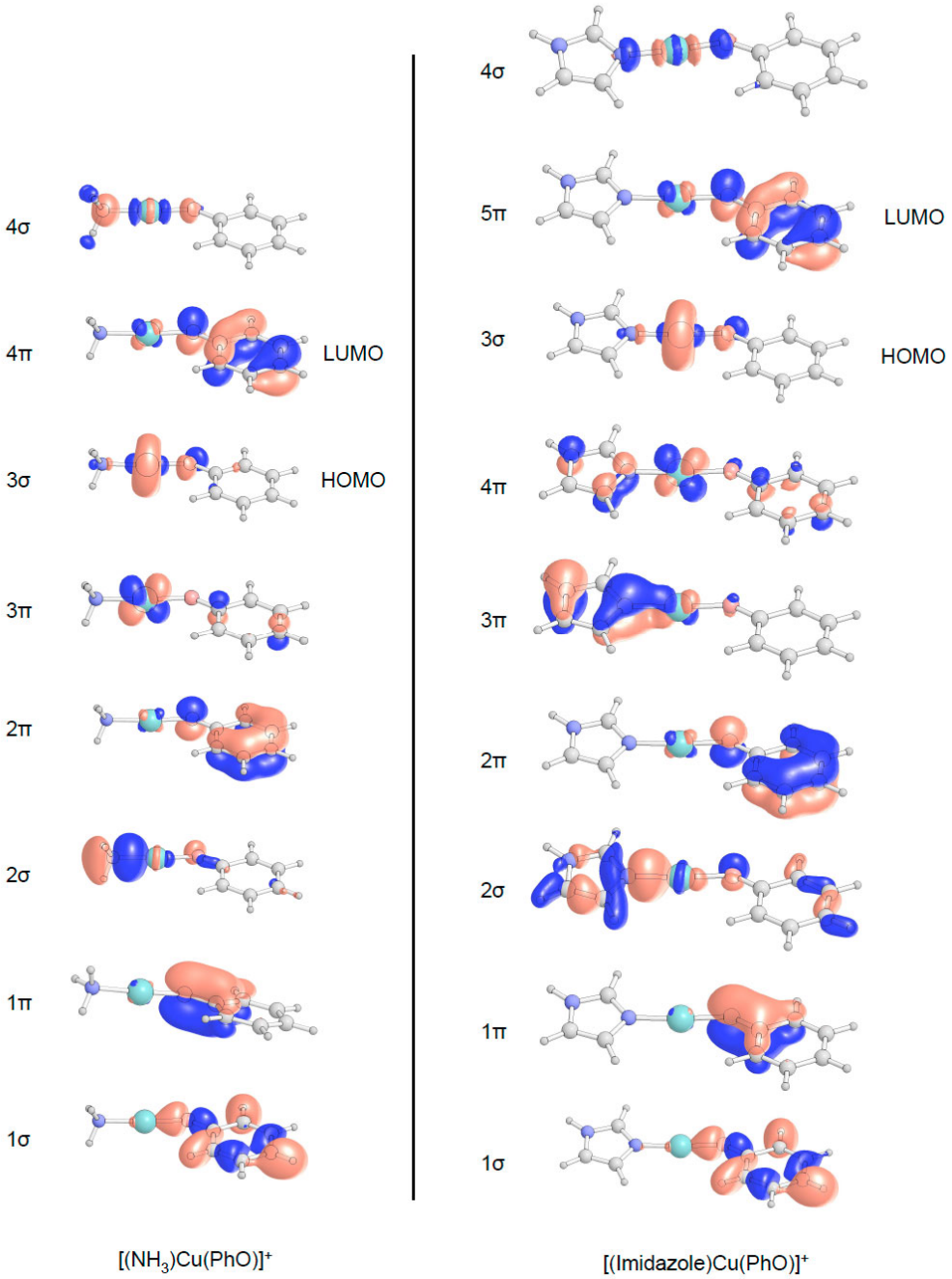

Figure S11. Isomers of complexes **2** and **3** (ZPVE corrected relative energies in eV).

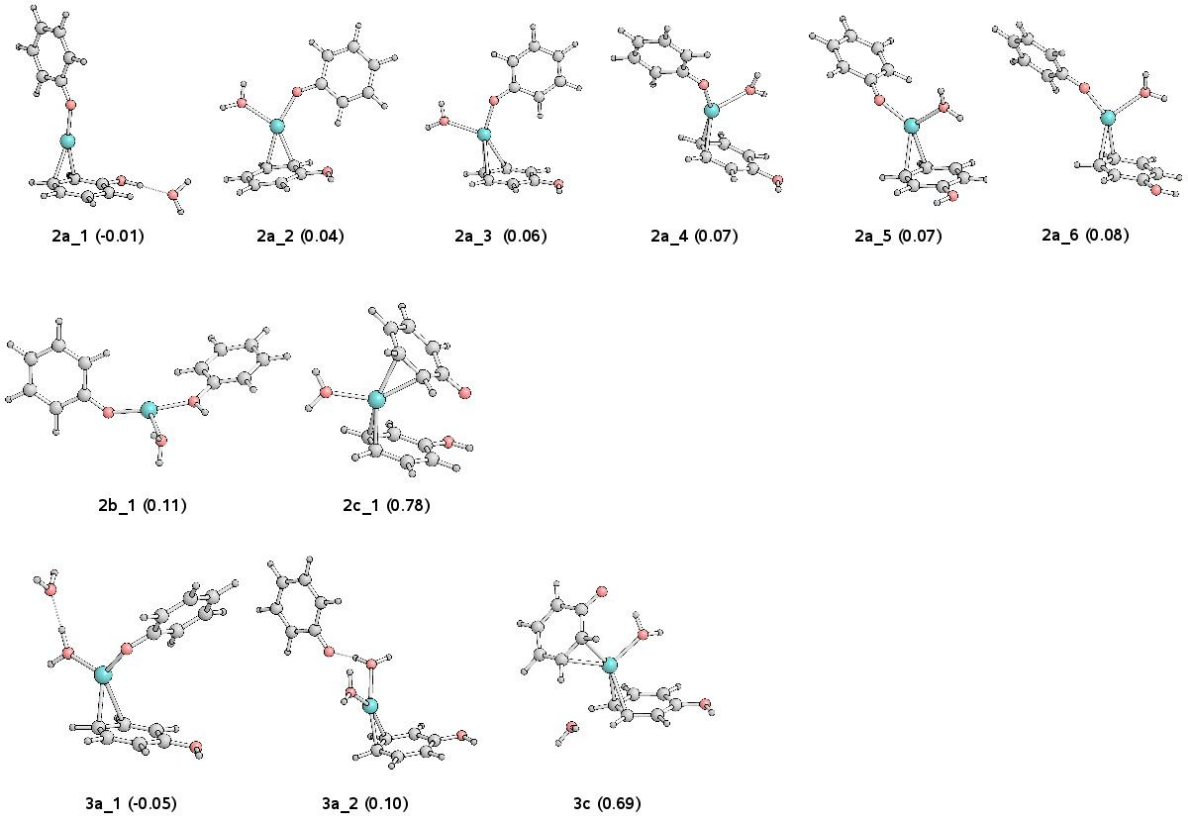

Figure S12. Isomers of complex **4**, and $[Cu(PhO)(PhOH)(NH_3)_2]^+$ optimized structures (ZPVE corrected relative energies in eV).

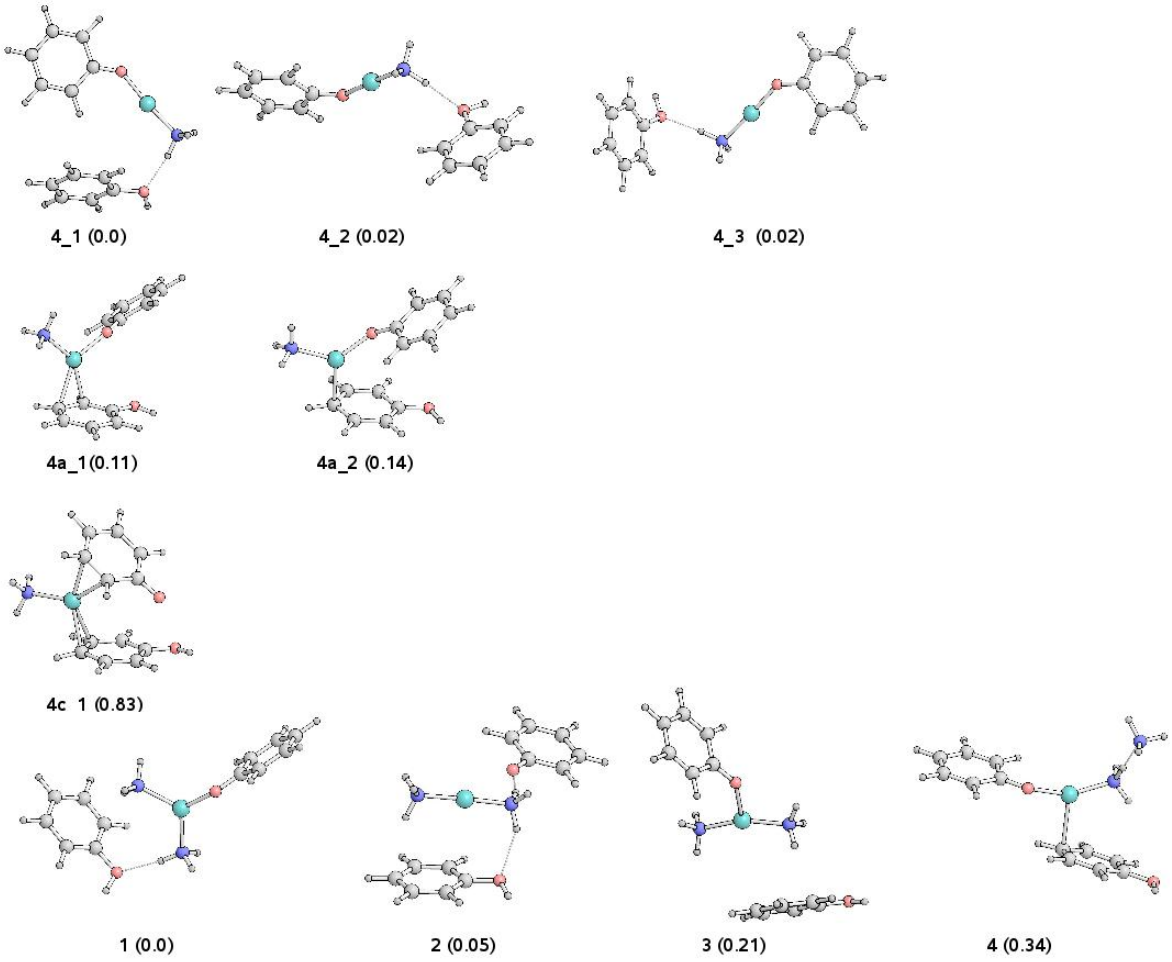

Figure S13. Isomers of complexes **5** and **6** (ZPVE corrected relative energies in eV).

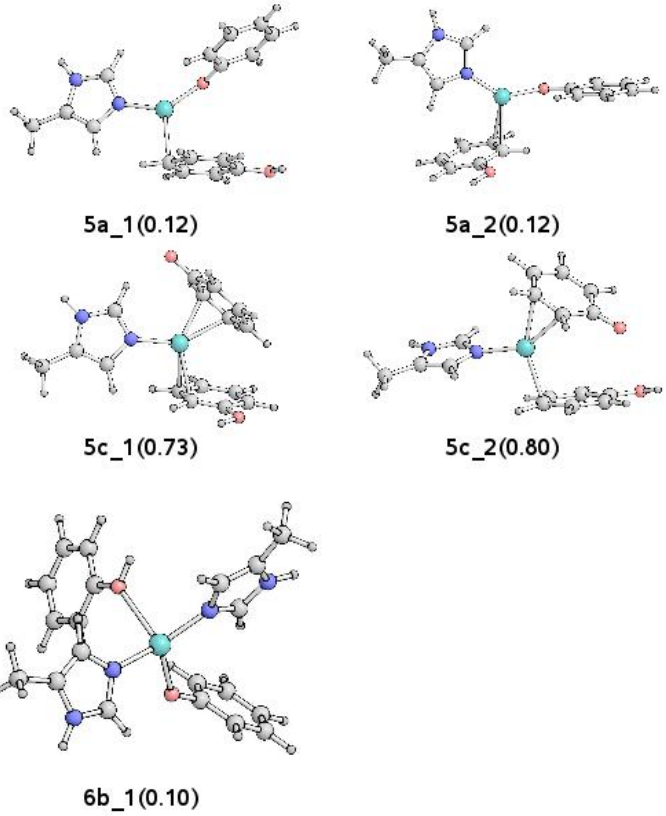

Figure S14. Isomers complex **6**b characterized at the B3LYP-D/TZVP level together with their stability relative to the global minimum (in eV).